REPORT DOCUMENTATION PAGE

Form Approved
OMB No. 0704-0188

1. REPORT DATE *(DD-MM-YYYY)*	**2. REPORT TYPE**	**3. DATES COVERED** *(From - To)*
12/08/2011	Final Report	9/15/2010 to 9/14/2011

4. TITLE AND SUBTITLE

Superoleophobic yet Superhydrophilic surfaces for continuous liquid-liquid separation.

5a. CONTRACT NUMBER

5b. GRANT NUMBER
FA9550-10-1-0523

5c. PROGRAM ELEMENT NUMBER

6. AUTHOR(S)

Dr. Anish Tuteja

5d. PROJECT NUMBER

5e. TASK NUMBER

5f. WORK UNIT NUMBER

7. PERFORMING ORGANIZATION NAME(S) AND ADDRESS(ES)

University of Michigan,
Division of Research Development and
Administration,
503 Thompson St, Ann Arbor, MI, 48109

8. PERFORMING ORGANIZATION REPORT NUMBER

10-PAF05652

9. SPONSORING / MONITORING AGENCY NAME(S) AND ADDRESS(ES)

Air Force Office of Scientific Research,
875 N. Randolph St, Room 3112,
Arlington, VA, 22203.

10. SPONSOR/MONITOR'S ACRONYM(S)

AFOSR

AFRL-OSR-VA-TR-2012-0800

12. DISTRIBUTION / AVAILABILITY STATEMENT

Approved for public release; distribution unlimited.

13. SUPPLEMENTARY NOTES

14. ABSTRACT

There is a critical need to develop new energy-efficient solutions for the separation of oil-water mixtures, including those stabilized b surfactants. Traditional membrane-based separation technologies for oil-water mixtures are energy-intensive and further limited, either b fouling or the inability of a single membrane to separate all types of oil-water mixtures. The ideal membrane to effect gravity-driven separatio of oil-water mixtures is expected to be both hydrophilic and oleophobic, in air and when submerged under water. Such membranes would allov the higher density liquid (water) to flow through, while retaining the lower density liquid (oil). However, as water possesses a significantl higher surface tension than various oils, most membranes that prevent the permeation of oils, also prevent the permeation of water. In this wor we report the first-ever reconfigurable membranes that, counter-intuitively, are both superhydrophilic (i.e., water contact angles ≅ 0°) *an* superoleophobic (i.e., oil contact angles > 150°). These membranes were designed through the systematic tailoring of membrane porosity an the membrane-water interfacial energy. The developed fouling-resistant membranes are able to separate all types of oil-water mixtures, with 99% separation efficiency, using a single membrane. Further, we have engineered the first-ever apparatus for continuous, solely gravity-drive separation of surfactant-stabilized oil-water emulsions, with a separation efficiency ≥ 99.9%.

15. SUBJECT TERMS

Oil-water separation, Membranes, Switchable surfaces, Non-wetting surfaces

16. SECURITY CLASSIFICATION OF: Unclassified			**Standard Form 298 (Rev. 8-98)** Prescribed by ANSI Std. Z39.18	**18. NUMBER OF PAGES**	**19a. NAME OF RESPONSIBLE PERSON** Anish Tuteja
a. REPORT UU	**b. ABSTRACT** UU				**19b. TELEPHONE NUMBER** *(include area code)* 734-615-2972

Final Project Report: Superoleophobic yet Superhydrophilic surfaces for continuous liquid-liquid separation.

Grant Number: FA9550-10-1-0523

PI: Dr. Anish Tuteja
Department of Materials Science and Engineering,
University of Michigan

Date: December 8, 2011.

Submitted to Dr. Charles Y-C. Lee,
Air Force Office of Scientific Research (AFOSR)
Email: charles.lee@afosr.af.mil

Executive Summary: There is a critical need to develop new energy-efficient solutions for the separation of oil-water mixtures, including those stabilized by surfactants. In this work we report the first-ever reconfigurable membranes that, counter-intuitively, are both superhydrophilic (i.e., water contact angles ≅ 0°) *and* superoleophobic (i.e., oil contact angles > 150°). These fouling-resistant membranes are able to separate all types of oil-water mixtures, with > 99% separation efficiency, using a single membrane. Further, we have engineered the first-ever apparatus for continuous, solely gravity-driven separation of surfactant-stabilized oil-water emulsions, with a separation efficiency ≥ 99.9%. Results from this proposal will lead to two publications, one of which has already been submitted (currently under review), while the other one is in preparation. The project involved two undergraduate students, one graduate student and a postdoctoral research associate. Results from this proposal have been presented in five invited lectures.

Several recent events, including the Deepwater Horizon oil-spill in the Gulf of Mexico, have highlighted the difficulty of effective oil-water separation. Efficient, cost-effective processes for oil-water separation, especially in the presence of dispersants (or surfactants), are greatly desired (*1*). Surfactant-stabilized mixtures of oil and water are classified by the diameter (d) of the dispersed phase as: i) free oil and water, if $d > 150$ μm, ii) a dispersion, if 20 μm $< d <$ 150 μm, or iii) an emulsion, if $d < 20$ μm. Conventional gravity separators and skimming techniques are incapable of separating emulsions (*2*).

Membrane-based technologies are attractive for *demulsification* i.e., the conversion of an emulsion to a free oil-water mixture, because they are relatively energy-efficient, cost-effective, and applicable across a wide range of industrial effluents (*2*). However, for complete oil-water *separation*, demulsification is typically followed by either gravity separation or skimming (*3*).

In most membrane literature (*4-11*), membranes are classified as either hydrophobic or hydrophilic. Their wettability by oil is often not specified because, in nearly all cases, such membranes are oleophilic, i.e., Young's contact angle (*12*) with oil $\theta_{oil} < 90^{o}$. Hydrophobic (or superhydrophobic (*10, 11, 13*)) and oleophilic membranes, which preferentially allow the passage of oil, are most often used in energy-intensive cross-flow filtration systems (*4, 7, 8*) as they are unsuitable for gravity-driven oil-water separation (*14*). Further, during demulsification,

hydrophobic (or superhydrophobic) membranes are easily fouled by oil (*7, 8*). Alternatively, although hydrophilic membranes can be used for gravity-driven demulsification, and are more resistant to fouling (*2*), they are not suitable for the separation of free oil–water mixtures or water-in-oil emulsions, as both oil and water can easily permeate through the membranes.

As many as three different phases (oil, oil-in-water or water-in-oil emulsion, and water) may co-exist in oil-water mixtures (*15, 16*). To affect gravity-driven separation of all types of oil-water mixtures, in a single step, the ideal separation membrane is expected to be both hydrophilic (or superhydrophilic) and oleophobic (or superoleophobic), both in air and when submerged under water. However, a membrane that is oleophobic in air typically loses its oleophobicity under water and vice-versa (*17, 18*).

Despite numerous natural superhydrophobic surfaces (*19, 20*), due to the low surface tension values for oils, there are no naturally-occurring, superoleophobic surfaces, i.e., surfaces for which $\theta^* > 150°$. Here, θ^* refers to the apparent contact angle of oil, i.e., the contact angle for oil on a textured surface. In recent work, we (*21-23*) and others (*24-27*) have explained how *re-entrant surface texture*, in conjunction with surface chemistry and roughness, can be used to design superoleophobic surfaces.

Most surfaces that are superoleophobic are also superhydrophobic *(22-24)*. This is due to the higher surface tension of water, which results in $\theta_{water} > \theta_{oil}$. A few studies have reported counter-intuitive surfaces with $\theta_{water} < \theta_{oil}$ (*28-32*). These reports typically utilized specific interaction between water and the substrate to lower the solid-liquid interfacial tension (γ_{sl}). However, with one exception (*32*), all such surfaces were oleophilic, with $\theta_{oil} < 90°$. Herein, we report novel hygro-responsive surfaces (from the Greek prefix '*hygra*' meaning liquid (*27*)) that,

for the first time, are superhydrophilic ($\theta_{water} \cong 0^o$) and superoleophobic ($\theta^*_{oil} > 150°$), both in air and under water.

The systematic design of membranes for oil-water separation requires the parameterization of two important physical characteristics: i) the surface porosity – which affects the rate of permeation of one phase (e.g., water) through the membrane, and ii) the breakthrough pressure ($P_{breakthrough}$) – the maximum pressure difference across the membrane below which the membrane can prevent the permeation of (or retain) the second phase (e.g., oil).

In our recent work (*21, 22*), we discussed the spacing ratio D^*, which provides a dimensionless measure of surface porosity. For substrates possessing a cylindrical texture, such as those considered here, $D^* = (R+D)/R$, where R is the radius of the cylinders and $2D$ is the inter-cylinder spacing. Higher D^* indicates higher porosity and therefore, higher permeation rate for the contacting liquid. Higher D^* also indicates higher apparent contact angles (θ^*) for the repelled liquid, provided the applied pressure difference $P_{applied} < P_{breakthrough}$ (*21, 22*). We (*22*) also discussed the robustness factor A^*, which is the ratio of $P_{breakthrough}$ and a reference pressure $P_{ref} = 2\gamma_{lv}/l_{cap}$. Here, $l_{cap} = \sqrt{\gamma_{lv}/\rho g}$ is the capillary length for the liquid, ρ is the liquid density and g is the acceleration due to gravity. P_{ref} is approximately the minimum possible pressure that may be applied on a membrane by commonly occurring liquid droplets or puddles (*22*). As a result, any membrane with $A^* \leq 1$ for a given liquid cannot prevent the liquid from permeating through it, while values of $A^* >> 1$ imply a high resistance to liquid permeation. For surfaces possessing a cylindrical texture, the robustness factor is given by (*21, 22*):

$$A^* = \frac{P_{breakthrough}}{P_{ref}} = \frac{Rl_{cap}}{D^2}\frac{(1-\cos\theta)}{(1+2(R/D)\sin\theta)} \quad (1)$$

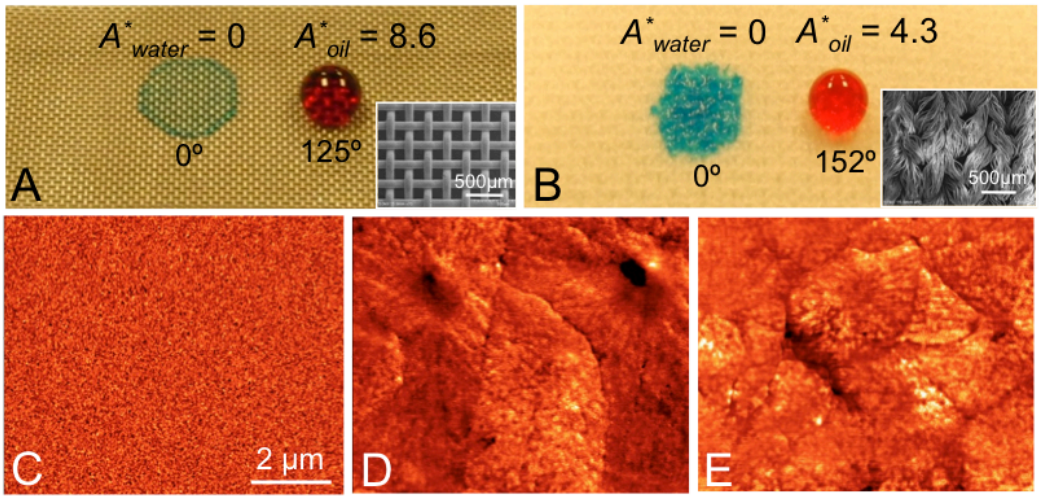

Figure 1. A and **B.** Droplets of water (dyed blue) and rapeseed oil (dyed red) on stainless steel mesh 100 and polyester fabric surfaces, respectively. Both surfaces have been dip-coated with 20 wt% fluorodecyl POSS + x-PEGDA blend. The insets in **A** and **B** illustrate the morphology of the dip-coated mesh and fabric surfaces, respectively. **C, D** and **E.** AFM phase images of x-PEGDA, 10 wt% fluorodecyl POSS + x-PEGDA blend, and 20 wt% fluorodecyl POSS + x-PEGDA blend surfaces, respectively. The phase angle scale for the images **C, D** and **E** ranges from 0°–115°, 0°–25° and 0°–21°, respectively.

Figs. 1*A* and 1*B* show the wetting behavior of water (γ_{lv} = 72.1 mN/m) and rapeseed oil (γ_{lv} = 35.7 mN/m) on a stainless steel mesh 100 (*33*) (inset Fig. 1*A*) and polyester fabric (inset Fig. 1*B*), each dip-coated with a 20 wt% fluorodecyl POSS (*34*) + x-PEGDA blend (cross-linked poly(ethylene glycol) diacrylate). For a spin-coated 20 wt% fluorodecyl POSS + x-PEGDA blend surface (γ_{sv} = 10.5 mN/m), the advancing contact angle for rapeseed oil $\theta_{oil,adv}$ = 88º. This yields A^*_{oil} values of 8.6 and 4.3 for rapeseed oil on the mesh and fabric membranes, respectively. As D^*_{fabric} (6) > D^*_{mesh} (2.2), the observed apparent advancing contact angle on the dip-coated fabric ($\theta^*_{oil,adv}$ = 152°) is higher than that on mesh 100 ($\theta^*_{oil,adv}$ = 125°). However, despite their low surface energy, water readily permeates through both the fabric and mesh membranes, with θ^*_{water} = 0°. This surprising observation is a direct consequence of the surface reconfiguration induced by the contacting water droplet, as discussed below.

Figs. 1*C*-1*E* present AFM phase images of x-PEGDA and two fluorodecyl POSS blends, in air. While crystalline domains are absent on the neat x-PEGDA surface (Fig. 1*C*), the surfaces of both 10 wt% and 20 wt% (Figs. 1*D* and 1*E*) blends are completely covered with crystalline domains of fluorodecyl POSS. This indicates significant surface segregation of the POSS molecules, as may be expected due to their extremely low surface energy (*23*). This surface migration leads to a rapid decrease in both dispersive (γ_{sv}^{d}) and polar components (γ_{sv}^{p}) of the blend surface energy.

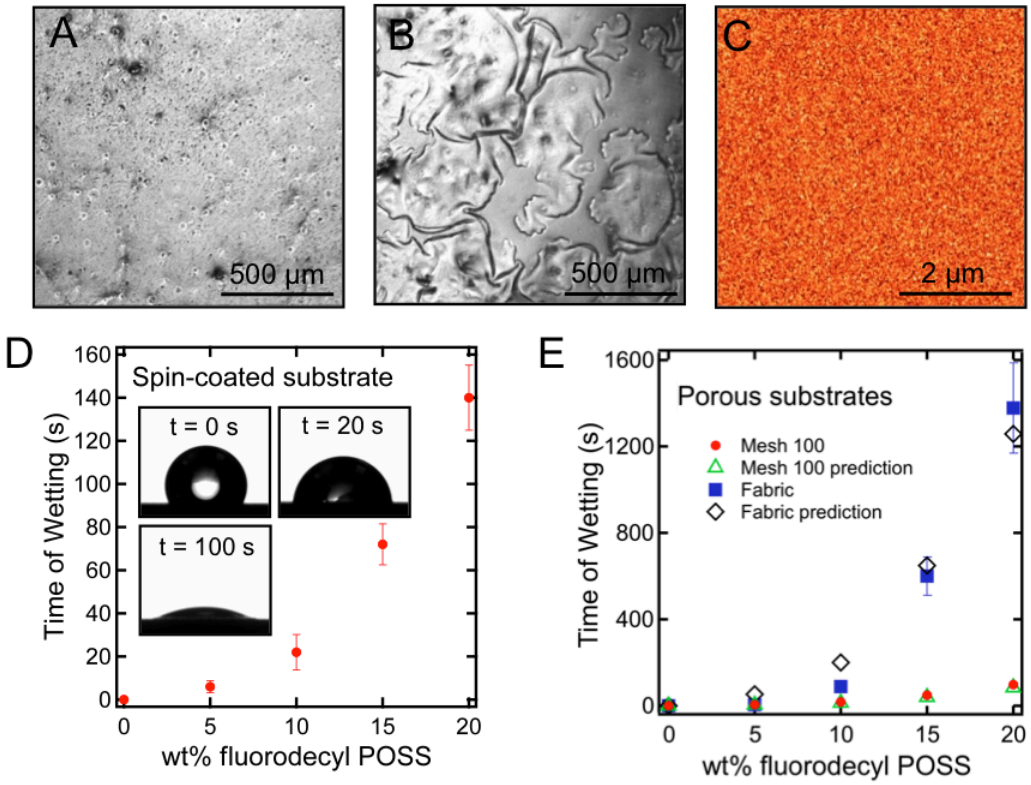

Figure 2. A and **B.** Optical microscopy images of 20 wt% fluorodecyl POSS + x-PEGDA blend surface in air and under water, respectively. **C.** *In-situ*, under water, AFM phase image of 20 wt% fluorodecyl POSS + x-PEGDA blend surface. The phase angle scale for this image ranges from 0°–112°. **D** and **E.** Time of wetting (ToW) of water on fluorodecyl POSS + x-PEGDA blends for different spin-coated and porous substrates, respectively. The insets in **D** show the time-dependant decrease in contact angle for a water droplet on a 20 wt% fluorodecyl POSS + x-PEGDA surface, due to surface reconfiguration. The time of wetting predictions on the mesh 100 and the fabric membranes match closely with experimental measurements, as shown in **E**.

Figs. 2*A* and 2*B* display optical images of spin-coated surfaces of 20 wt% fluorodecyl POSS + x-PEGDA, in air and under water, respectively. In air, the surface is relatively rough with several

fluorodecyl POSS aggregates. However, under water, fluorodecyl POSS aggregates disappear to reveal a smoother surface (with a few wrinkles) that is indicative of surface reconfiguration. PEGDA chains reconfigure to increase their interfacial area with water and facilitate enthalpic gains through hydrogen bonding. Surface reconfiguration is further confirmed by the absence of large crystalline domains in the *in-situ*, under water AFM phase image (Fig. 2*C*). We conducted multiple water wetting-drying cycles and found that this surface reconfiguration is reversible. Surface energy analysis of the wet surface suggests that it is equivalent to an x-PEGDA blend with ~ 0.4–1.5 wt% fluorodecyl POSS.

Addition of fluorodecyl POSS causes a systematic increase in the time required for surface reconfiguration, as evident from the increased time of wetting (ToW) for water on spin-coated fluorodecyl POSS + x-PEGDA surfaces (*35*) (Fig. 2*D*). We define ToW as the time required for the water contact angle on a surface to decrease from its initial value and reach 0º. We also measured ToW for water on the porous mesh and fabric membranes (Fig. 2*E*). On these surfaces, we define ToW as the time required for the water droplet to imbibe into the membrane.

Membrane imbibition is not instantaneous for surfaces with reconfigurable chemistry. Instead, the water-air interface progressively penetrates into the surface texture (*36*) and water permeates through the membrane once the robustness factor $A^*_{water} \leq 1$. From Eq. 1, for mesh 100, $A^*_{water} = 1$ when $\theta_{water} = 18º$. Our ToW measurements on dip-coated meshes match closely with the time required for $\theta_{water,adv}$ to decrease from its initial value to 18º (Fig. 2*E*). However, ToW for water on the dip-coated fabrics was found to be significantly higher. This is because water has to progressively wet multiple fibers during imbibition.

Conventional membrane separation of oil-water emulsions relies on size exclusion, the viscosity difference between immiscible phases, or the coalescence of the emulsified phase. Very

few reports in membrane separation (*32, 37*) and in microfluidics (*38, 39*) have utilized the difference in capillary forces acting on the individual phases as the primary mechanism to separate emulsions or dispersions. We term this methodology as *Capillary Force-based Separation* (CFS). In CFS, the wetting phase permeates through the membrane, while the non-wetting phase is retained. From Eq. 1, the breakthrough pressure required to force the non-wetting phase through a membrane already saturated by the wetting phase is:

$$P_{breakthrough} = \frac{2R\gamma_{12}}{D^2}\frac{(1-\cos\theta')}{(1+2(R/D)\sin\theta')} \tag{2}$$

Here, γ_{12} is the interfacial tension between the wetting and the non-wetting phase, while θ' is the contact angle of the non-wetting phase on the solid surface, both of which are completely immersed in the wetting phase. When applied pressure $P_{applied} < P_{breakthrough}$, only the wetting phase permeates through the membrane.

We utilize CFS in this work for three reasons. First, CFS provides a very high quality permeate as the non-wetting phase is entirely retained on the membrane (*38, 39*). Second, the inherent self-repairing (*39, 40*) nature of CFS renders the permeate quality resistant to pressure perturbations. Third, CFS combines both demulsification and separation into a single unit-operation, unlike most techniques used for emulsion separation (*5, 6, 9*). For a CFS–based system to work effectively, it is necessary to ensure that the wetting phase encounters the membrane. There are several techniques to achieve this goal: gravity-driven (if the wetting phase has a higher density than the non-wetting phase), electrostatic (if the wetting phase is a polar liquid) (*41*), forced convection (*4, 7, 8*), etc. In this work we demonstrate two proof-of-concept prototypes that solely utilize gravity to engender emulsion separation.

Figs. 3*A* and 3*B* show solely gravity-driven CFS of a Sodium Dodecyl Sulfate (SDS; hydrophilic-lipophilic balance HLB = 40) stabilized hexadecane-in-water emulsion (50 vol% hexadecane; see materials and methods). Hexadecane droplet size distribution indicates a wide-range of droplet diameters (100 nm < d_{oil} < 1000 μm), with the highest number fraction of droplet diameters in the range of 10–20 μm. The separation apparatus consists of a mesh 400 (2*D* = 37.5 μm) (*42*), dip-coated with 20 wt% fluorodecyl POSS + x-PEGDA blend sandwiched between two vertical glass tubes. The emulsion is added to the upper tube (Fig. 3*A*). Within minutes, the water-rich permeate passes through the membrane while the hexadecane-rich retentate is retained above the membrane (Fig. 3*B*). Membrane oleophobicity, when submerged under water, is necessary for the separation of hexadecane-in-water emulsions (inset in Fig. 3*A*). Thermogravimetric analyses (TGA) indicate that the permeate contains ~ 0.1 wt% hexadecane, while the retentate contains ~ 0.1 wt% water (Fig. 3*C*). This high separation efficiency is further confirmed by comparing the transmittance of the feed emulsions with that of the permeates, as well as, density measurements. Optical image analysis of the droplet size distribution in the permeate indicates that the membrane removes virtually all hexadecane droplets exceeding 40 μm in diameter. Additional experiments showed that we can similarly separate, with > 99% efficiency, hexadecane-in-water emulsions containing 10 vol% and 30 vol% hexadecane.

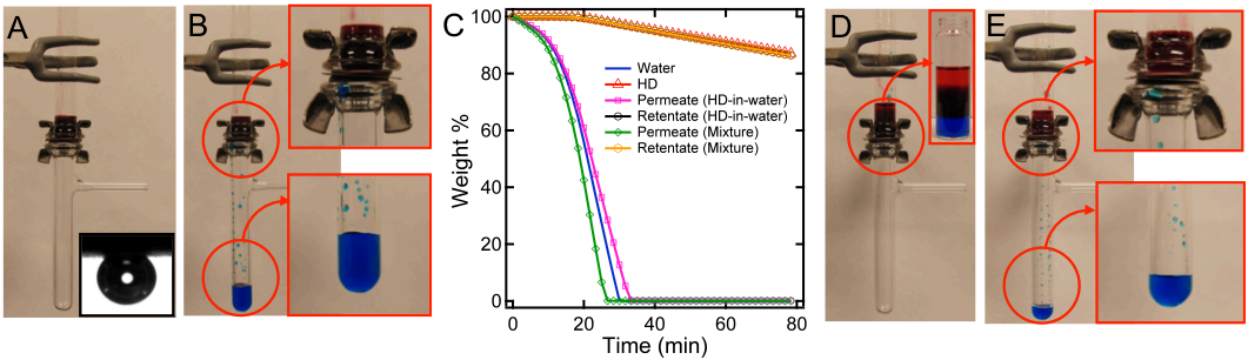

Figure 3. A. A gravity-driven CFS apparatus with a 50:50 v:v hexadecane-in-water emulsion in the upper tube above the membrane. The inset shows the contact angle of hexadecane on a surface spin-coated with 20 wt% fluorodecyl POSS + x-PEGDA blend, submerged in water containing dissolved SDS (1 mg/mL). The contact angle was measured to be 120°. **B.** After membrane surface reconfiguration, water-rich permeate passes through the membrane while hexadecane-rich retentate is retained above the membrane. **C.** Thermogravimetric analyses of the permeate and the retentate from separation of hexadecane-in-water emulsion and the 4 component mixture (water, hexadecane, hexadecane-in-water emulsion and water-in-hexadecane emulsion). The data for pure water and as-obtained hexadecane (HD) are also shown for comparison. **D.** The 4 component mixture in the upper tube of the separation apparatus, above the membrane. The inset shows a larger quantity of the feed in a glass vial to clearly depict the presence of different phases. **E.** After membrane surface reconfiguration, water-rich permeate passes through the membrane while hexadecane-rich retentate is retained above the membrane. In **A, B, D** and **E**, water is dyed blue and hexadecane is dyed red.

We can similarly separate, with > 99% efficiency, multiple Polysorbate80 (PS80; HLB = 15) and Span80 (HLB = 4.3) stabilized water-in-hexadecane emulsions. Membrane oleophobicity, both in air and under water, is critical for separating water-in-hexadecane emulsions.

Figs. 3*D* and 3*E* exhibit the separation of a mixture containing 4 components: water, hexadecane, water-in-hexadecane emulsion and hexadecane-in-water emulsion. Again, mesh 400 dip-coated with 20 wt% fluorodecyl POSS + x-PEGDA blend successfully separated this mixture into a permeate containing ~ 0.1 wt% hexadecane and a retentate containing ~ 0.1 wt% water, as confirmed by thermogravimetric analyses (Fig. 3*C*). To our knowledge, this is the first ever report on solely gravity-driven separation of surfactant-stabilized emulsions into highly pure constituents. Further, the dip-coating based membrane fabrication process is easy to scale-up, and we have developed an apparatus to separate several liters of oil-water mixtures (see Fig. 4A).

For the separation apparatus shown in Figs. 3*A* and 3*D*, the maximum height of the liquid column before breakthrough ($h_{breakthrough}$) can be obtained using Eq. 2 ($P_{breakthrough} = \rho g h_{breakthrough}$, where ρ is the density of the liquid). For the 50:50 v:v hexadecane-in-water emulsions, $\theta'_{oil,adv}$ = 120° (inset in Fig. 3*A*), γ_{12} = 4.0 mN/m, and $h_{breakthrough}$ is predicted to be 2.3 cm. Similarly, $h_{breakthrough}$ for the 30:70 v:v water-in-hexadecane emulsion is predicted to be 2.4 cm. These values closely match experimentally measured values of 2 cm and 2.2 cm for the hexadecane-in-water and water-in-hexadecane emulsions, respectively. Our analysis also indicates that after the separation, the surfactant fractionates into both the water-rich and the hexadecane-rich phases, depending upon its relative solubility in each phase.

In the design discussed above, oil accumulates above the membrane over time and will eventually breakthrough once operating height $h > h_{breakthrough}$. Therefore, we have developed a continuous oil-water separation apparatus, with two CFS-based operations in parallel, utilizing a superhydrophilic and oleophobic membrane at the bottom and a hydrophobic and oleophilic membrane on the sidewall. Fig. 4*A* shows an image of our apparatus during the separation of the 30:70 v:v water-in-hexadecane emulsion. TGA (Fig. 4*B*) indicates that the water-rich permeate contains ~ 0.1 wt% hexadecane, while the hexadecane-rich permeate contains ~ 0.1 wt% water, which is the limit of detection for the TGA. Karl Fischer analysis indicates that the hexadecane-rich permeate contains ~ 25±8 ppm water, which is comparable to the solubility of water in hexadecane (~ 30 ppm at 25ºC). Thus, in this case, our membrane allows for nearly complete removal of the insoluble water droplets.

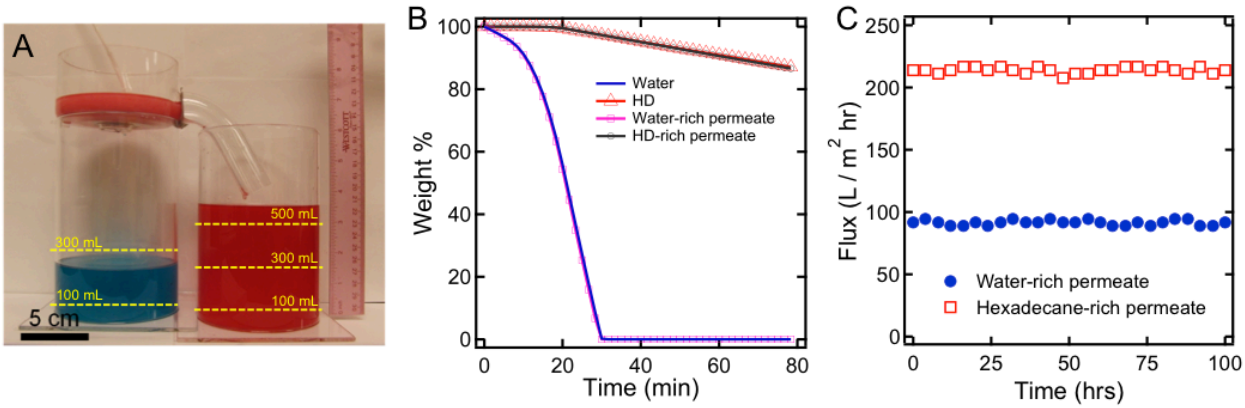

Figure 4. A. An image of the scaled-up apparatus used for the continuous separation of water-in-hexadecane emulsions. The emulsion is fed at a constant flux using a syringe pump. The superhydrophilic and oleophobic mesh 400 was dip-coated with a 20 wt% fluorodecyl POSS + x-PEGDA blend, while the hydrophobic and oleophilic mesh 400 was dip-coated with Desmopan 9370A (γ_{sv} = 35.6 mN/m). During continuous separation, water-rich permeate continuously passes through the superhydrophilic and oleophobic membrane, while hexadecane-rich permeate continuously passes through the hydrophobic and oleophilic membrane. Water is dyed blue and hexadecane is dyed red. **B.** TGA data for both the permeates. The data for pure water and as-obtained hexadecane (HD) are also shown for comparison. **C.** Measured fluxes for both the permeates as a function of time.

Analysis of the hexadecane-rich permeate also indicates that at least 99.8% of water droplets with diameter < 20 μm are removed during separation. For membranes used in this separation $2D$ = 37.5 μm. Thus, it is clear that the membrane allows for the removal of dispersed phase droplets that are significantly smaller than the membrane pore size.

To our knowledge, this is the first demonstration of continuous, solely gravity-driven CFS of oil-water emulsions. Fluxes of water-rich and hexadecane-rich permeates through the membranes were measured to be 90 L/m^2-hr and 210 L/m^2-hr, respectively. These values are comparable to those reported in membrane separation literature for dead-end filtration (*44, 45*) and cross-flow filtration (*4, 5, 7, 8*), where separation was engendered using an energy intensive, externally applied pressure difference, as opposed to the sole use of gravity in this report. Further, the fluxes did not decline over a period of 100 hours (Fig. 4*C*), indicating that the membranes are highly resistant to fouling by oil. This observation is in contrast to the flux decline observed for most hydrophobic membranes (*7, 8*). Membrane wettability, and the

significantly larger pore sizes of the membranes used here, compared to those used traditionally (*4, 6, 8, 9*), are expected to be two major contributors towards the observed fouling-resistance.

The flux for the water-rich permeate during continuous separation is significantly lower than that predicted by the Hagen-Poiseuille relation (*43*). This is because for water-in-oil emulsions, the flux is limited by the sedimentation velocity of the water droplets. Based on this understanding, the flux for water was predicted to be ~ 83 L/m^2-hr, which closely matches experimental results. Further, as the flux of water-rich permeate is limited only by the sedimentation velocity, it is independent of the pore diameter, for all pore diameters $2D >> 4.5$ μm. Indeed, experimentally, we obtained the same flux for water using both mesh 400 ($2D$ = 37.5 μm) and mesh 500 ($2D$ = 30.5 μm) during continuous separation. However, a membrane with a smaller pore diameter, such as mesh 500, has a higher value for $P_{breakthrough}$ and is, therefore, more resistant to pressure perturbations.

In conclusion, we have developed the first-ever superhydrophilic *and* superoleophobic membranes based on hygro-responsive coatings that reversibly become superhydrophilic when contacted by water. These membranes are oleophobic both in air and when submerged under water. Consequently, CFS-based unit operations utilizing these membranes can separate, with > 99% efficiency, free oil and water, oil-in-water emulsions, water-in-oil emulsions, and any combination of these phases. We have also engineered, for the first time, an apparatus that utilizes two CFS-based operations in parallel, to achieve continuous, solely gravity-driven separation of oil–water emulsions, with a separation efficiency ≥ 99.9 %.

Experimental Details:

Materials. Poly(ethylene glycol) diacrylate (PEGDA) with a number average molecular weight $M_n \sim$ 700 Da and its cross-linker, 2-hydroxy-2-methyl propiophenone (Darocur 1173), were

obtained from Sigma Aldrich. Poly(methyl methacrylate) (PMMA) of weight average molecular weight $M_w \sim 35{,}000$ Da was obtained from Scientific Polymer Products, Inc. Tecnoflon BR9151 fluoroelastomer was obtained from Solvay Solexis. Desmopan 9374 polyurethane was obtained from Bayer Material Science. 1H,1H,2H,2H-Heptadecafluorodecyl Polyhedral Oligomeric SilSequioxane (fluorodecyl POSS) was synthesized as described elsewhere (*23*). Asahiklin AK-225 solvent was obtained from Structure Probe, Inc. Rapeseed oil, hexadecane, tetrahydrofuran (THF), methylene blue (blue dye), oil red-o (red dye), sodium dodecyl sulfate (SDS), Polysorbate80 (PS80), Span80 and glass slides, were obtained from Fisher Scientific. Stainless steel meshes of mesh size 100 (R = 56.5 mm, $2D$ = 138 mm, D^* = 2.2), 400 (R = 12.5 mm, $2D$ = 37.5 mm, D^* = 2.5), 500 (R = 10.2 mm, $2D$ = 30.5 mm, D^* = 2.5) were obtained from McMaster Carr. The mesh number refers to the number of openings per inch. The fabric Anticon 100 (R_{bundle} = 150 mm, $2D_{bundle}$ = 300 mm, R_{fiber} = 5 mm, $2D_{fiber}$ = 20 mm, D^* = 6) was obtained from VWR. Silicon wafers were obtained from the clean room at the University of Michigan.

Dip-coating, spin-coating, and cross-linking of synthesized coatings. 100 mg/ml solutions of PEGDA, Darocur1173 and fluorodecyl POSS were prepared in Asahiklin AK-225. PEGDA:Darcour1173 ratio was maintained at 95:5 wt:wt. Fluorodecyl POSS concentrations studied were 0, 0.5, 1, 2, 5, 10, 15 and 20 wt%. 50mg/ml solutions of PMMA, 10 mg/ml solutions of PMMA with 40 wt% fluorodecyl POSS, and 10 mg/ml solutions of Tecnoflon with 50 wt% fluorodecyl POSS were prepared in Asahiklin AK-225. 10 mg/ml solutions of Desmopan were prepared in THF. Small pieces of mesh and fabric (2 cm long x 2 cm wide) were dip-coated by immersing in the desired solution for 10 min and subsequently dried with nitrogen gas at room temperature for 5 min. The non-textured substrates (silicon wafers, 2 cm long x 2 cm wide, and glass slides, 2 cm long x 3 cm wide) were spin-coated using Specialty Coating

Systems Spincoater G3P–8 for 30 s at 250–2000 RPM. After dip-coating or spin-coating, the PEGDA containing surfaces were cross-linked for 5 min using UVP XX-40S UV bench lamp (l = 254 nm). The mesh and fabric pore diameters 2D remained almost unaffected after dip-coating, with the thickness of the dip-coated layer varying between 100 nm – 1 mm.

Oil-water emulsions. 10:90 v:v, 30:70 v:v and 50:50 v:v hexadecane-in-water emulsions were prepared by mixing water and hexadecane using a stir bar (at 700-1200 RPM) with 0.1-0.5 mg of SDS/mL of emulsion, while 10:90 v:v, 20:80 v:v and 30:70 v:v water-in-hexadecane emulsions were prepared with 0.1-0.3 mg of PS80/mL of emulsion and 0.1-0.3 mg of Span80/mL of emulsion. We determined whether an emulsion is hexadecane-in-water or water-in-hexadecane by measuring the electrical resistance with a multimeter. A KDScientific KDS-200 syringe pump was used to deliver the feed emulsions during continuous separation.

Contact angle measurements. All contact angle measurements (in air and under water) were conducted using Ramé-Hart 200-F1 goniometer. All contact angles reported in this work were measured by advancing or receding a small volume of liquid (~ 2 mL) onto the surface using a 2 mL micrometer syringe (Gilmont). At least three measurements were performed on each substrate. Typical error in measurements was ±2º.

Microscopy. Tapping-mode atomic force microscopy (AFM) was conducted in air and under water using a Veeco Innova instrument. Veeco TESPA tips were used for imaging in air, while Veeco SNL-10C tips were used for imaging under water. The thickness of the spin-coated films was determined using an AFM line-scan across a scratched location. To ensure conformal coating, scanning electron microscopy (SEM) of the dip-coated surfaces was conducted using Hitachi SU8000 at 5 kV. Optical microscopy of the dry and wet spin-coated surfaces was conducted using an Olympus BH-2 optical microscope.

Thermogravimetric analysis, Karl Fischer analysis, transmittance and dynamic light scattering. The water content in both the hexadecane-rich and the water-rich phases after separation was measured using a Perkin Elmer Pyris 1 TGA. Approximately 50 mg of the sample was heated from room temperature to 105°C at a rate of 5°C/s, and the temperature was held constant at 105°C for 60 minutes. Note that the boiling point of hexadecane is 287ºC. The loss in weight of water was used to estimate the purity of the water-rich phase. The loss in weight of the hexadecane-rich phase was compared with the loss in weight of the as-obtained hexadecane to estimate the purity of the hexadecane-rich phase. The water content in the hexadecane-rich phase was also determined by injecting samples ranging from 10 μL to 0.6 mL into an EM Science AquaStar C3000 Titrator for coulometric Karl Fischer titration analysis (ASTM D6304). The transmittance of the feed emulsions and the permeates was measured using a Cary 50 Bio UV-vis spectrophotometer. The size distribution of the dispersed phase with droplet sizes less than 1 mm was determined by dynamic light scattering using a Malvern Zetasizer Nano ZS instrument.

Publications submitted and in-preparation:

1. "*Hygro-responsive membranes: A novel methodology for effective oil-water separation*", Arun K. Kota, Gibum Kwon, Wonjae Choi, Joseph M. Mabry, and Anish Tuteja. Submitted.
2. "*Membranes for the continuous separation of immiscible alkane-alcohol mixtures*", Mark K. Peter, Arun K. Kota, Joseph M. Mabry, and Anish Tuteja. In preparation.

Presentations: Results from this work were presented at the following venues:

1. Invited Lecture, "*Hygro-Responsive Membranes: A new approach for Oil-Water Emulsion Separation*", American Chemical Society National Meeting, August 28 – Sep. 1, 2011, Denver, CO.

2. Invited Lecture, "*Hygro-Responsive Membranes: A new approach for Oil-Water Emulsion Separation*", Dow Corning Limited, Midland, MI, March 1, 2011.
3. Invited Lecture, "*Hygro-Responsive Membranes: A new approach for Oil-Water Emulsion Separation*", Department of Chemical Engineering, University of Toledo, Toledo, OH, Feb. 3, 2011.
4. Invited Lecture, "*Hygro-Responsive Membranes: A new approach for Oil-Water Emulsion Separation*" in ACS Division of Polymer Chemistry's conference on "Silicon Containing Polymers and Composites", Dec. 11-14, San Diego, CA.
5. Invited Lecture, "*Hygro-Responsive Membranes: A new approach for Oil-Water Emulsion Separation*" Department of Physics, Michigan State University, East Lansing, MI, November 18, 2010

References

1. E. Kintisch, An Audacious Decision in Crisis Gets Cautious Praise. *Science* **329**, 735 (2010).
2. M. Cheryan, N. Rajagopalan, Membrane processing of oily streams. Wastewater treatment and waste reduction. *Journal of Membrane Science* **151**, 13 (1998).
3. A. Hong, A. G. Fane, R. Burford, Factors affecting membrane coalescence of stable oil-in-water emulsions. *Journal of Membrane Science* **222**, 19 (2003).
4. M. Hlavacek, Break-up of Oil-in-Water Emulsions Induced by Permeation through a Microfiltration Membrane. *Journal of Membrane Science* **102**, 1 (1995).
5. D. Z. Sun, X. D. Duan, W. X. Li, D. Zhou, Demulsification of water-in-oil emulsion by using porous glass membrane. *Journal of Membrane Science* **146**, 65 (1998).
6. S. Hoffmann, W. Nitsch, Membrane coalescence for phase separation of oil-in-water emulsions stabilized by surfactants and dispersed into smallest droplets. *Chem. Eng. Technol.* **24**, 22 (2001).
7. A. Maartens, E. P. Jacobs, P. Swart, UF of pulp and paper effluent: membrane fouling-prevention and cleaning. *Journal of Membrane Science* **209**, 81 (2002).
8. B. Hu, K. Scott, Influence of membrane material and corrugation and process conditions on emulsion microfiltration. *Journal of Membrane Science* **294**, 30 (2007).
9. M. Kukizaki, M. Goto, Demulsification of water-in-oil emulsions by permeation through Shirasu-porous-glass (SPG) membranes. *Journal of Membrane Science* **322**, 196 (2008).
10. L. Feng *et al.*, A Super-Hydrophobic and Super-Oleophilic Coating Mesh Film for the Separation of Oil and Water *Angewandte Chemie International Edition* **43**, 2012 (2004).
11. D. Tian, X. Zhang, X. Wang, J. Zhai, L. Jiang, Micro/nanoscale hierarchical structured ZnO mesh film for separation of water and oil. *Physical Chemistry Chemical Physics* **13**, 14606 (2011).
12. T. Young, An Essay on the Cohesion of Fluids. *Philos. Trans. R. Soc. London* **95**, 65 (1805).
13. J. Yuan *et al.*, Superwetting nanowire membranes for selective absorption. *Nature Nanotechnology* **3**, 332 (2008).
14. This is because water naturally settles below the oil and against the membrane due to its higher density, forming a barrier layer that prevents oil permeation.
15. T. Tadros, R. Izquierdo, J. Esquena, C. Solans, Formation and stability of nano-emulsions. *Adv. Colloid Interface Sci.* **108**, 303 (2004).
16. J. Meunier, *Physics of amphiphilic layers*. (1987).
17. Y. C. Jung, B. Bhushan, Wetting Behavior of Water and Oil Droplets in Three-Phase Interfaces for Hydrophobicity/philicity and Oleophobicity/philicity, *Langmuir* **25**, 14165 (2009).
18. L. Lin *et al.*, Bio-Inspired Hierarchical Macromolecule–Nanoclay Hydrogels for Robust Underwater Superoleophobicity. *Advanced Materials* **22**, 4826 (2010).
19. T. L. Sun, L. Feng, X. F. Gao, L. Jiang, Bioinspired surfaces with special wettability. *Accounts Chem. Res.* **38**, 644 (2005).
20. D. Quere, Non-sticking drops. *Rep Prog Phys* **68**, 2495 (2005).
21. W. Choi *et al.*, Fabrics with Tunable Oleophobicity. *Advanced Materials* **21**, 2190 (2009).

22. A. Tuteja, W. Choi, J. M. Mabry, G. H. McKinley, R. E. Cohen, Robust omniphobic surfaces. *Proceedings of the National Academy of Sciences of the United States of America* **105**, 18200 (2008).
23. A. Tuteja *et al.*, Designing superoleophobic surfaces. *Science* **318**, 1618 (2007).
24. A. Ahuja *et al.*, Nanonails: A simple geometrical approach to electrically tunable superlyophobic surfaces. *Langmuir* **24**, 9 (2008).
25. L. Cao, T. P. Price, M. Weiss, D. Gao, Super Water- and Oil-Repellent Surfaces on Intrinsically Hydrophilic and Oleophilic Porous Silicon Films. *Langmuir* **24**, 1640 (2008).
26. B. Leng, Z. Shao, G. de With, W. Ming, Superoleophobic Cotton Textiles. *Langmuir* **25**, 2456 (2009).
27. A. Marmur, From Hygrophilic to Superhygrophobic: Theoretical Conditions for Making High-Contact-Angle Surfaces from Low-Contact-Angle Materials. *Langmuir* **24**, 7573 (2008).
28. A. Vaidya, M. K. Chaudhury, Synthesis and Surface Properties of Environmentally Responsive Segmented Polyurethanes. *J. Colloid Interface Sci.* **249**, 235 (2002).
29. H. Sawada, Y. Ikematsu, T. Kawase, Y. Hayakawa, Synthesis and surface properties of novel fluoroalkylated flip-flop-type silane coupling agents. *Langmuir* **12**, 3529 (1996).
30. S. J. Hutton, J. M. Crowther, J. P. S. Badyal, Complexation of Fluorosurfactants to Functionalized Solid Surfaces: Smart Behavior. *Chemistry of Materials* **12**, 2282 (2000).
31. J. A. Howarter, J. P. Youngblood, Self-Cleaning and Anti-Fog Surfaces via Stimuli-Responsive Polymer Brushes. *Advanced Materials* **19**, 3838 (2007).
32. J. A. Howarter, J. P. Youngblood, Amphiphile grafted membranes for the separation of oil-in-water dispersions. *J. Colloid Interface Sci.* **329**, 127 (2009).
33. The mesh number refers to the number of openings per inch.
34. J. M. Mabry, A. Vij, S. T. Iacono, B. D. Viers, Fluorinated polyhedral oligomeric silsesquioxanes (F-POSS). *Angew. Chem.-Int. Edit.* **47**, 4137 (2008).
35. This is due to a reduction in the interfacial area between PEGDA chains and the contacting water droplet with increasing fluorodecyl POSS concentration.
36. This is because for any membrane, if the liquid does not permeate through its pores, the solid-liquid-air composite interface equilibrates at a location on the membrane where the local texture angle (ψ) is equal to the Young's contact angle θ.
37. N. P. Tirmizi, B. Raghuraman, J. Wiencek, Demulsification of water/oil/solid emulsions by hollow-fiber membranes. *Aiche J.* **42**, 1263 (1996).
38. J. G. Kralj, H. R. Sahoo, K. F. Jensen, Integrated continuous microfluidic liquid-liquid extraction. *Lab Chip* **7**, 256 (2007).
39. D. E. Angelescu, B. Mercier, D. Siess, R. Schroeder, Microfluidic Capillary Separation and Real-Time Spectroscopic Analysis of Specific Components from Multiphase Mixtures. *Anal. Chem.* **82**, 2412 (2010).
40. I. Chatzis, F. A. L. Dullien, Dynamic Immiscible Displacement Mechanisms In Pore Doublets - Theory Versus Experiment. *Journal of Colloid and Interface Science* **91**, 199 (1983).
41. T. Ichikawa, K. Itoh, S. Yamamoto, M. Sumita, Rapid demulsification of dense oil-in-water emulsion by low external electric field: I. Experimental evidence. *Colloids and Surfaces A: Physicochemical and Engineering Aspects* **242**, 21 (2004).

42. We used the superhydrophilic and oleophobic meshes here because they allow us to systematically tune the pore sizes. Our superhydrophilic and superoleophobic fabrics also show a similar performance.
43. G. K. Batchelor, *An introduction in fluid dynamic by G. K. Batchelor*. (U.P, Cambridge, 1970).
44. T. C. Arnot, R. W. Field, A. B. Koltuniewicz, Cross-flow and dead-end microfiltration of oily-water emulsions - Part II. Mechanisms and modelling of flux decline. *J. Membr. Sci.* **169**, 1 (2000).
45. A. B. Koltuniewicz, R. W. Field, T. C. Arnot, Cross-flow and dead-end microfiltration of oily-water emulsion - 1. Experimental-study and analysis of flux decline. *Journal of Membrane Science* **102**, 193 (1995).